

Performance of concrete modified with SCBA and GGBFS subjected to elevated temperature

Satish Muralidhar Palaskar* and Gaurang R. Vesmawala^a

Department of Civil Engineering, SVNIT, Surat, India

(Received May 2, 2020, Revised May 21, 2020, Accepted September 12, 2020)

Abstract. This research paper presents the outcomes in terms of mechanical and microstructural characteristics of binary and ternary concrete when exposed to elevated temperature. Three parameter were taken into account, (a) elevated temperature (i.e., 200, 400, 600 and 800°C) (b) binary concrete with cementitious material sugarcane bagasse ash (SCBA) and ground granulated blast furnace slag (GGBFS) replacement percentage (i.e., 0, 15, 20, 25 and 30%) and (c) ternary concrete with cementitious material SCBA and GGBFS replacement percentage (i.e., 0, 15, 20, 25 and 30%). A total of 285 standard cube specimens (150 mm × 150 mm × 150 mm) containing Ordinary Portland Cement (OPC), SCBA, and GGBFS were made. These specimens then exposed to several elevated temperatures for 2 h, afterward is allowed to cool at room temperature. The following basic physical, mechanical, and microstructural characteristics were then determined and discussed. (a) mass loss ratio, (b) ultrasonic pulse velocity (UPV) (c) physical behavior, (d) compressive strength, and (e) field emission scanning electron microscope (FESEM). It was found that compressive strength increases up to 400°C; beyond this temperature, it decreases. UPV value and mass loss decrease with increase in temperature as well as the change in color and crack were observed at a higher temperature.

Keywords: concrete; sugarcane bagasse ash; ground granulated blast furnace slag; elevated temperature; residual strength; microstructural properties

1. Introduction

Concrete is commonly consumed as the primary structural material in construction due to multiple benefits like strength, durability, production convenience, and non-combustible characteristics as compared with other construction material. When used in building, concrete structural members must meet the necessary fire safety specification as per building codes as fire is among the worst environmental condition that structures can be exposed. Appropriate fire safety measures are, therefore, an essential aspect of the design of the building for the structural members. Fire safety steps were evaluated for structural members in the way of fire resistance, which is the duration for which structural members prevent resistance concerning structural stability as well as temperature transmission. Concrete typically offers the best properties as compared with other building materials for fire resistance. This outstanding resistance to fire is mostly related to the constituent elements of concrete, i.e., cement and aggregate. The behavior of concrete subjected to

*Corresponding author, Research Scholar, E-mail: satishpalaskar@gmail.com

^a Ph.D., Associate Professor

fire depend mostly on thermal, mechanical, and deformation properties of which it is made.

Khan and Abbas (2016) obtained four concrete mixes consuming several amounts of GGBFS and silica fume and 43 grade OPC. A concrete cube of 100 mm was cast and exposed to a peak temperature 100, 200, 300, 400, 500, 600, and 700°C for the duration of 1, 2, 3, and 7 h. The compressive strength of GGBFS based concrete rises up to 200°C. Afterward, it reduces steadily, but it does not disintegrate or splinter. Silica fume based concrete showed poor performance when subjected to elevated temperature. It was also noted that greater heating temperatures resulted in a greater mass loss (Khan and Abbas 2016). Ashteyat *et al.* (2014) developed a statistical model to forecast the remaining mechanical properties of post heated self-compacting concrete using non-destructive testing (NDT). This test was performed before and after exposure to heating. The specimen was heated for 300, 400, 500, and 600°C for 2 h. The model generated from the test results revealed an excellent fit of the data engaged and helped as a suitable tool for forecasting post-heating remaining properties (Ashteyat *et al.* 2014). Yadollahi *et al.* learned the influence of elevated temperature on pumice based geopolymer concrete, which was exposed to 100, 200, 300, 400, 500, 600, 700, and 800°C for 3 h. Compressive strength loss rises with a rise in temperature. The specimen, which was grey, turned whitish accomplished by the appearance of cracks as temperature increases from 600°C to 800°C (Yadollahi *et al.* 2015). The inner steam load is the main cause of the spalling of HPC. Concurrently, the temperature rising rate and restrained condition of the concrete component also play an important role in spalling as noted by Dong Xiangjan *et al.* when concrete subjected to fire (Dong *et al.* 2008). Chan *et al.* determined the compressive strength of HPC when subjected to higher temperatures up to 800°C and shows higher residual strength (Chan *et al.* 2000). Zheng *et al.* studied compressive strength properties and microstructure of reactive powder concrete and revealed that compressive strength first increases and then decreases due to deterioration of microstructure (Zheng *et al.* 2012). Shaikh studied the effect of different slag content on the residual compressive strength, and physical properties of fly ash-slag blended geopolymer at elevated temperatures of 400, 600, and 800°C. All mixes showed significant damage in terms of cracking after exposure to 800°C as compared with 400 and 600°C. SEM also shows higher porosity at 800°C. After exposure to elevated temperature, the calcite/CSH peaks disappeared, and new phases of nepheline and gehlenite were formed at 800°C. Reduction in compressive strength was observed at all exposure (Shaikh 2018). Ozawa and Morimoto noted that there is an increase in permeability when fiber reinforced concrete subjected to high temperature (Ozawa and Morimoto 2014). Sideris *et al.* determined the performance of fiber-reinforced concrete when subjected to high temperatures. Explosive spalling and linearly reducing compressive strength were observed as temperature goes on increasing (Sideris *et al.* 2009). Rafat Siddique and Kaur examined the influence of elevated temperature on concrete containing GGBFS. Up to 100°C, there was no significant deterioration of mechanical properties. Mass loss was significant between 200 to 350°C. Degradation of concrete microstructure due to the modification of hydrates was observed (Siddique and Kaur 2012). Salau *et al.* learned the effect of recycled coarse aggregate at 200, 400, and 600°C for 2 h. From 100 to 200°C drop in strength observed, then increase in strength from 200 to 450°C, and again strength drop occurred up to 600°C. Slight surface hairline cracks were noticed as the temperature approached 400°C (Salau *et al.* 2015). Hachemi and Ounis learned the efficiency of concrete obtained from crushed sand at raised temperatures. Specimens were heated at ambient temperature 150, 250, 400, 600, and 900°C. Result exhibited that there will be insignificant variations in the physical characteristics of concrete prepared using crushed sand (Hachemi and Ounis 2017). Drzymala *et al.* carried different tests on HPC exposed to raised temperatures and found that heating up to 300°C increases strength (Drzymala *et al.* 2017). Ko *et al.* investigated

changes in the microstructure of concrete, moisture transfer, and internal pressure of concrete subjected to elevated temperature and found that moisture transfer was closely related to the temperature profiles resulting from the characteristics of pore structures, which are the main passages for moisture (Ko *et al.* 2011). Liu *et al.* investigated the mechanical behavior of concrete exposed to 100, 200, 300, 400, 600, and 800°C. The concrete below 400°C shows surface color similar to room temperature. After 600 and 800°C, there are some micro cracks on the surface. The width of cracks increases with an increase in temperature. There is a remarkable deterioration of concrete strength (Liu *et al.* 2018). Gencil *et al.* studied the mechanical properties of concrete containing haematite evaluated using the fuzzy logic model at elevated temperature. Different proportions of haematite were used to fabricate the concrete, which is subjected to 25, 200, 400, 600, and 800°C. Whose output results show good correlation with experimental results (Gencil *et al.* 2013). Tai *et al.* noted reduced peak stress; however, peak strain raises when the temperature increases significantly. Compressive strength increases when the specimen is heated from 200 to 300°C (Tai *et al.* 2011). Belouadah *et al.* found 400 and 600°C as a critical temperature range when used glass powder in concrete (Belouadah *et al.* 2018). Sahani *et al.* used GGBFS, fly ash to replace natural sand and OPC. The thermo-mechanical study was performed on the specimen exposed to 200, 400, 600, 800, and 1000°C for 4 h duration. Additional by-product enhanced weight loss, their permeability, and higher residual compressive strength even up to 800°C. Microstructural study exhibited improvement in density even at high temperatures (Sahani *et al.* 2019). Poon *et al.* noted that 45% and 23% of compressive strength retained when fiber reinforced concrete exposed to 600 and 800°C, respectively (Poon *et al.* 2004). Ma *et al.* investigated the influence of elevated temperature on modified lightweight expanded clay aggregate. The temperature was 200, 400, 600, 800, 1000, and 1200°C for 3 h. Test results show that all the modified concrete specimens were unbroken even at a temperature of 1200°C with no spalling as well as maintained sound mechanical properties (Ma *et al.* 2018). Chen *et al.* used recycled coarse aggregate in the concrete, which was subjected to 20, 200, 300, 400, 500, 600, and 800°C temperatures. The test result indicates that as temperature increases surface color changes, mass loss ratio increases, elastic modulus, and peak stress decreases, and peak strain increases (Chen *et al.* 2019). Zhao *et al.* used recycled coarse aggregate in concrete, which was exposed to 20, 200, 400, 600, and 800°C temperatures. The experimental results indicated that both compressive strength and modulus of elasticity of recycled coarse aggregate concrete decreases continuously with increasing temperature, whereas peak strain increases rapidly (Zhao *et al.* 2017).

Wu *et al.* used a thermocouple sensor to detect temperature and found that outside temperature was higher as compared with the core temperature when high strength concrete subjected to elevated temperature (Wu *et al.* 2019). Le *et al.* measured temperature at three different depths, i.e., at specimen surface, at centreline, and 21 mm from the surface using five thermocouples for each specimen. They observed a reasonable degree of consistency among the measured temperature for each heat flux. The recorded temperature along the two radial lines at corresponding depths also had good agreement, further confirming the uniform heat flux boundary condition (Le *et al.* 2018).

Previous studies on the performance of concrete incorporating different cementitious material after exposure to elevated temperature have focussed on mechanical and microstructural properties. However, results are different to compare with each other and can even produce inconsistent conclusions because of differences in cementitious materials, specimen dimensions, and testing conditions. Further studies are, therefore, still needed to extend the data and clarify the effect of SCBA and GGBFS. Until now the mechanical and microstructural studies of binary and ternary concrete modified with SCBA and GGBFS in the temperature range from room temperature to

Table 1 Chemical properties of SCBA and GGBFS

Properties	SiO ₂	Al ₂ O ₃	Fe ₂ O ₃	CaO	MgO	SO ₃
SCBA	82.53	12.62	0.60	2.34	1.04	0.001
GGBFS	34.12	18.95	0.23	35.46	8.2	0.45

800°C has not been reported. This is not only unique scope for improving the amount of consumption of agriculture and industrial by-product but also enhance the weightage of alternative material for special industrial functions such as concrete structure near furnaces, ovens, and steel plants.

The main objective of the current study is to explore the influence of the addition of SCBA and GGBFS on the residual properties of binary and ternary concrete and its microstructure at elevated temperature.

2. Experimental work

2.1 Material

The Ordinary Portland cement of 53 grade confirming to IS12269-1987 was used in this work. Sugarcane bagasse ash was obtained from Prasad Sugar and allied agro-products Ltd. Ahmednagar, Maharashtra. The SCBA obtained is heated in a muffle furnace at 700°C for 2 h and then allowed to cool at room temperature. Before using, it was grinded to make it fine. GGBFS is obtained from Guru Corporation, Ahmedabad Gujarat. The chemical properties of SCBA and GGBFS are shown in Table 1. Natural sand having maximum size 4.75 mm was used as fine aggregate whereas coarse aggregate of maximum size 20 mm and 12.5 mm in the proportion of 60:40 were used in the concrete mix. Both the fine aggregate and coarse aggregate are according to the requirement of IS383:1970.

2.2 Methodology

Preliminary experiments were carried out to ensure sustainability performance by checking compressive strength at 28 days before elevated temperature exposure. Then elevated temperature performance was measured in terms of mass loss, change in color, cracks on surfaces, UPV value as per IS 13311(Part1)-1992 and compressive strength as per IS 516-1959 of the specimen after exposure to elevated temperatures (200, 400, 600 and 800°C) for 2 h duration. Surface color and thermal cracks on the surface were observed through visual inspection. FESEM investigations were also carried out on selected specimens to confirm the outcomes of test results at room temperature and at 400 & 800°C.

2.3 Details of mix proportion

Nineteen concrete mixes containing control mix were made as per IS 456-2000 to discover the effect of elevated temperature on SCBA and GGBFS based binary and ternary concrete. Control mix for M25 concrete with the ratio of 1:1.83:2.99 (cement: sand: aggregate) was designed consuming water-cement ratio (w/c) of 0.5 to attain cubic target mean strength of 31.6 MPa. All aggregate is used in saturated surface dry conditions. Weight batching was implemented for all

Table 2 Mix proportion and properties of concrete with and without SCBA and GGBFS

Mix ID	Cement (%)	SCBA (%)	GGBFS (%)	Property	Room temperature 25°C (RT)	200°C	400°C	600°C	800°C
P	100	0	0	Compressive strength (MPa)	37.39	41.29	45.62	30.11	14.18
				Mass loss (%)		3.20	7.01	9.22	10.02
				UPV (km/s)	4.63	4.14	3.25	2.13	1.56
				Density (kg/m ³)	2606	2638	2526	2416	2465
B15	85	15	0	Compressive strength (MPa)	41.15	42.45	46.52	32.56	15.65
				Mass loss (%)		3.18	7.21	9.38	9.94
				UPV (km/s)	4.52	4.20	3.59	2.23	1.78
				Density (kg/m ³)	2628	2566	2475	2409	2383
B20	80	20	0	Compressive strength (MPa)	37.31	38.42	42.20	27.89	12.51
				Mass loss (%)		3.10	7.41	9.36	9.89
				UPV (km/s)	3.47	4.32	3.02	1.87	1.13
				Density (kg/m ³)	2609	2513	2411	2384	2359
B25	75	25	0	Compressive strength (MPa)	35.24	36.01	39.95	26.17	12.10
				Mass loss (%)		3.22	7.33	8.97	10.50
				UPV (km/s)	4.38	4.15	3.05	1.56	1.02
				Density (kg/m ³)	2570	2499	2397	2371	2346
B30	70	30	0	Compressive strength (MPa)	30.56	29.42	34.62	23.51	11.31
				Mass loss (%)		3.35	7.28	8.81	10.84
				UPV (km/s)	4.39	4.10	2.95	1.31	0.98
				Density (kg/m ³)	2519	2475	2383	2349	2324
G15	85	0	15	Compressive strength (MPa)	40.82	41.23	43.89	33.36	15.34
				Mass loss (%)		3.42	7.62	8.93	10.32
				UPV (km/s)	4.50	4.12	2.81	1.80	1.13
				Density (kg/m ³)	2634	2608	2457	2441	2395
G20	80	0	20	Compressive strength (MPa)	37.94	38.02	40.36	30.42	14.36
				Mass loss (%)		3.49	7.55	9.92	10.64
				UPV (km/s)	4.45	4.05	2.72	1.58	0.91
				Density (kg/m ³)	2608	2596	2489	2433	2385
G25	75	0	25	Compressive strength (MPa)	36.21	36.94	38.91	29.96	13.48
				Mass loss (%)		3.49	7.49	9.78	10.66
				UPV (km/s)	4.47	3.90	2.70	1.49	0.88
				Density (kg/m ³)	2638	2555	2477	2430	2382
G30	70	0	30	Compressive strength (MPa)	34.67	35.98	36.44	28.44	12.89
				Mass loss (%)		3.51	7.44	9.86	10.29
				UPV (km/s)	4.48	3.87	2.68	1.32	0.78
				Density (kg/m ³)	2642	2568	2510	2380	2366

Table 2 Continued

Mix ID	Cement (%)	SCBA (%)	GGBFS (%)	Property	Room temperature 25°C (RT)	200°C	400°C	600°C	800°C
B10G05	85	10	05	Compressive strength (MPa)	40.02	41.25	42.03	33.62	16.13
				Mass loss (%)		3.50	7.23	9.27	10.31
				UPV (km/s)	4.49	4.09	3.29	2.01	1.20
				Density (kg/m ³)	2661	2480	2417	2347	2342
B10G10	80	10	10	Compressive strength (MPa)	35.49	37.93	35.82	29.18	14.13
				Mass loss (%)		3.52	7.79	9.64	10.38
				UPV (km/s)	4.51	4.13	3.07	1.73	0.85
				Density (kg/m ³)	2762	2491	2423	2367	2352
B10G15	75	10	15	Compressive strength (MPa)	34.98	35.69	36.20	27.51	12.93
				Mass loss (%)		3.38	7.63	9.36	10.41
				UPV (km/s)	4.50	4.10	3.00	1.79	0.92
				Density (kg/m ³)	2734	2511	2422	2372	2369
B10G20	70	10	20	Compressive strength (MPa)	35.11	36.02	37.98	28.47	13.02
				Mass loss (%)		3.17	7.78	9.55	10.38
				UPV (km/s)	4.49	4.04	2.81	1.70	0.86
				Density (kg/m ³)	2692	2522	2408	2360	2413
B15G05	80	15	05	Compressive strength (MPa)	38.00	39.17	39.94	30.75	14.14
				Mass loss (%)		3.27	7.43	9.59	10.84
				UPV (km/s)	4.45	4.00	2.90	2.10	1.68
				Density (kg/m ³)	2665	2546	2431	2377	2362
B15G10	75	15	10	Compressive strength (MPa)	33.70	34.39	35.23	27.93	12.57
				Mass loss (%)		3.35	7.53	9.91	10.96
				UPV (km/s)	4.41	4.12	2.82	1.96	1.37
				Density (kg/m ³)	2677	2565	2412	2345	2369
B15G15	70	15	15	Compressive strength (MPa)	33.62	32.69	33.44	23.82	11.38
				Mass loss (%)		3.43	7.33	10.5	10.64
				UPV (km/s)	4.36	4.30	3.03	2.26	1.89
				Density (kg/m ³)	2718	2565	2384	2348	2386
B20G05	75	20	05	Compressive strength (MPa)	32.50	33.51	34.12	24.57	11.30
				Mass loss (%)		3.52	7.8	10.13	10.89
				UPV (km/s)	4.48	4.21	3.10	3.02	1.50
				Density (kg/m ³)	2618	2610	2472	2393	2413
B20G10	70	20	10	Compressive strength (MPa)	31.29	35.18	35.44	28.51	13.51
				Mass loss (%)		3.61	8.16	10.02	10.85
				UPV (km/s)	4.50	4.19	2.75	1.85	0.96
				Density (kg/m ³)	2750	2482	2427	2404	2395

Table 2 Continued

Mix ID	Cement (%)	SCBA (%)	GGBFS (%)	Property	Room temperature 25°C (RT)	200°C	400°C	600°C	800°C
B25G05	70	25	05	Compressive strength (MPa)	30.84	31.50	32.69	23.86	10.74
				Mass loss (%)		3.38	8.00	10.31	10.94
				UPV (km/s)	4.43	4.02	2.98	2.10	1.10
				Density (kg/m ³)	2620	2562	2465	2399	2388

kinds of mixes. Table 2 shows the quantity of cement replaced by SCBA and GGBFS in different specimens. In whole experimental work, the cubic specimen of size 150 mm was prepared following IS516-1959 to obtain compressive strength.

2.4 Heating and cooling regime

The cube was cured in portable water for 28 days and then air-dried before being exposed to elevated temperature. An electric arc furnace in a forging factory at Ahmednagar Maharashtra was used. The furnace temperature was controlled by using an electronic temperature controller. The furnace was able to maintain a uniform temperature with a precision of $\pm 1^\circ\text{C}$. During heating and cooling, the furnace was closed entirely (except holes for the release of fumes). When the samples were put in the furnace, the internal temperature of the furnace was at room temperature. The overall heating rate was $4^\circ\text{C}/\text{min}$ (ISO/TR 15655 2003), the temperature was kept steady for 2 h after the maximum value attained (200, 400, 600, and 800°C) (Zheng *et al.* 2012). The cubes were then tested when cooled inside the furnace.

3. Result and discussion

3.1 Compressive strength

Cube compressive strength of all the mixes was evaluated at 28 days of water curing to check whether SCBA and GGBFS from a particular source are suitable or not for normal exposure. Both binary and ternary concrete exhibited a relatively similar trend of variation in results. Almost all replacement mixes could be able to achieve the target mean strength of 31.6 MPa at 28 days. Compressive strength was highly influenced by the percentage increase in SCBA and GGBFS. The variations of compressive strength with elevated temperature for 19 concrete mixes are shown in Table 2. It is found that all samples have an improved compressive strength until 400°C then reduces as temperature goes on rising. The early strength might result from the speeding up of the hydration process, and a successive reduction might result from the decomposition of cement paste, at 105°C , the capillary water, and free water vaporize (Khan and Abbas 2016). There will be an increase in compressive strength at 300°C , and at 450°C compressive strength decreases when the internal temperature was monitored by inserting thermocouples at different points (Drzymala *et al.* 2018).

Fig. 1(a) demonstrates the variation of compressive strength of binary concrete mixes containing SCBA. In the case of binary concrete containing 15% SCBA (B15 mix), compressive strength rises with a rise in temperature up to 400°C and then starts decreasing. It was also observed that at all

temperatures, compressive strength for the B15 mix was higher as compared with control concrete. Whereas compressive strength of 20, 25, and 30% SCBA (B20, B25, and B30 combinations) was lower as compared with the control mix at all variations of temperature. It was also observed that as the temperature increases up to 400°C rate of increase in compressive strength decreases with an increase in SCBA content. Fig. 1(b) demonstrates the variation of compressive strength of binary concrete containing GGBFS. In the case of concrete containing 15 and 20% GGBFS (G15 and G20 mix), the compressive strength rises with a rise in temperature up to 400°C and then starts reducing. But the rate of increase in strength is less as compared with control concrete, for G15 mix compressive strength was found to be the same up to 200°C as compare with control concrete. Compressive strength of G25 and G30 mix also rises with a rise in peak temperature up to 400°C and then starts reducing, but it was less as compared with control concrete. Fig. 2 demonstrates the variation of compressive strength of ternary concrete containing SCBA and GGBFS. In case of ternary concrete containing 10% SCBA & 5% GGBFS (B10G05 mix) and 15% SCBA & 5% GGBFS (B15G05 mix) shows better results at all temperature as compare with control concrete. Thus, concrete containing a higher percentage of SCBA and a lower percentage of GGBFS with a variation of temperature up to 400°C exhibited better results as compared with the control concrete. For 800°C heating period variation in compressive strength of all ternary mixes is much less as compared with the 600°C heating period. The maximum standard deviation is 3.61 MPa for the B15G15 mix at 600°C for control concrete; it was 3.04 MPa.

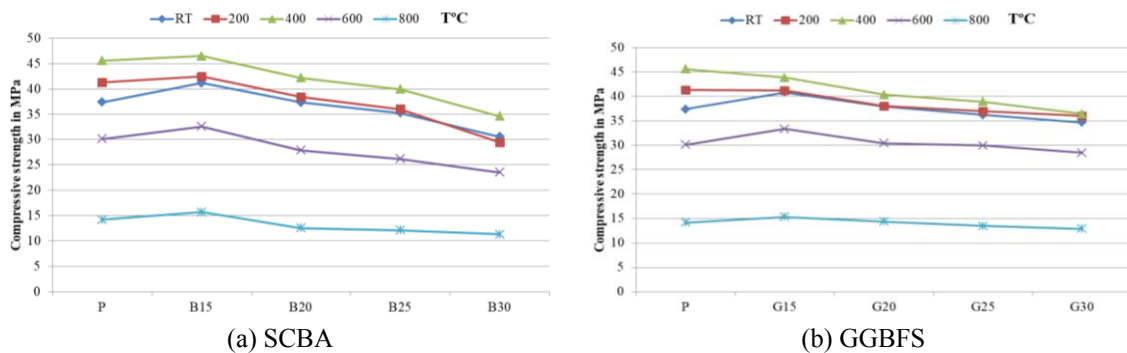


Fig. 1 Compressive strength for various binary mixes at elevated temperature

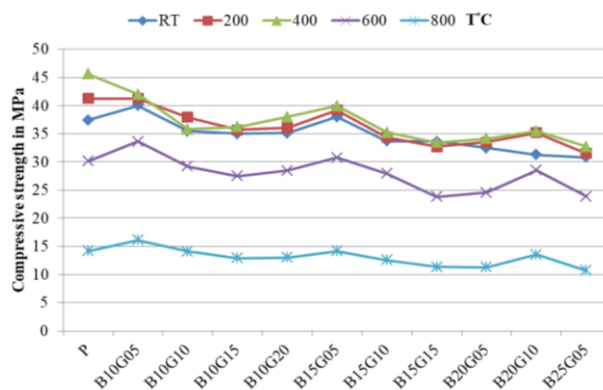


Fig. 2 Compressive strength for various ternary mixes of SCBA & GGBFS at elevated temperature

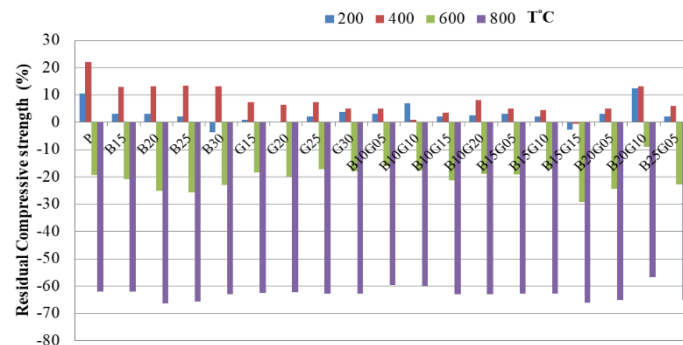


Fig. 3 Residual compressive strength for various binary and ternary mixes of SCBA and GGBFS at elevated temperature

For distinguishing the role of additives in concrete mixes, residual compressive strength, and rise in temperature has been shown in Fig. 3. At 200°C, an increase of 0.92-12.43% in compressive strength as compared to room temperature strength were observed. At 400°C, an increase of 0.92-22.01% in compressive strength as compared to room temperature strength were observed. At 600°C, a decrement of 8.88-29.15% in compressive strength as compared to room temperature strength was observed. At 800°C, a decrement of 56.82-66.47% in compressive strength as compared to room temperature strength were observed. Calcium hydroxide, which is one of the valuable compounds in cement paste, dissociates at around 400 to 600°C (Wu *et al.* 2019), causing shrinkage of concrete and affecting a more significant reduction in strength (Arioz 2007). The decomposition of $\text{Ca}(\text{OH})_2$ and C-S-H gel, especially at 800°C, maybe resulting in higher strength loss (Sahani *et al.* 2019).

3.2 Mass loss

Fig. 4 shows the percentage mass losses at 200, 400, 600, and 800°C temperature tested for 2 h. It has been observed that the mass loss of all concrete specimens increases sharply up to 400°C, afterwards, it increases marginally. It was also seen that mass loss of binary concrete containing SCBA was less as compared with binary concrete containing GGBFS at all temperatures. In the case of ternary concrete, mass loss was observed to be more for all specimens at all temperatures. The mass loss of concrete mixes is also found to increase with an increase in temperature. The maximum standard deviation is 65 gm. for the B30 mix at 800°C; for control concrete, it was 32 gm.

The primary changes taking place in concrete at a temperature lower than 600°C is the loss of physically absorbed and chemically bound water. The weight loss observed at 800°C exceeds the amount that can be accounted by water alone and is likely caused by the decomposition of aggregates and cement hydration products (Deshpande *et al.* 2019). Omer Arioz studied the effects of elevated temperature on properties of concrete and found higher weight loss for higher w/c ratio, which reveals that the water content of mixture increases with respect to w/c ratio (Arioz 2007).

Reduction in the mass loss was found to be 3.1 to 3.61% at 200°C, which increased from 7.01 to 8.16% for 400°C temperature. For 600°C and 800°C temperature, reduction in mass loss ranges from 8.81 to 10.5% and 9.89 to 10.96%, respectively. Reduction in the mass loss at 400°C temperature is more than twice than that of 200°C. Beyond 400°C, reduction in mass loss decreases as temperature will go on increasing. Maximum water in each concrete specimen evaporated during heating between 200°C and 400°C (Belouadah *et al.* 2018). Lowest mass loss was observed for

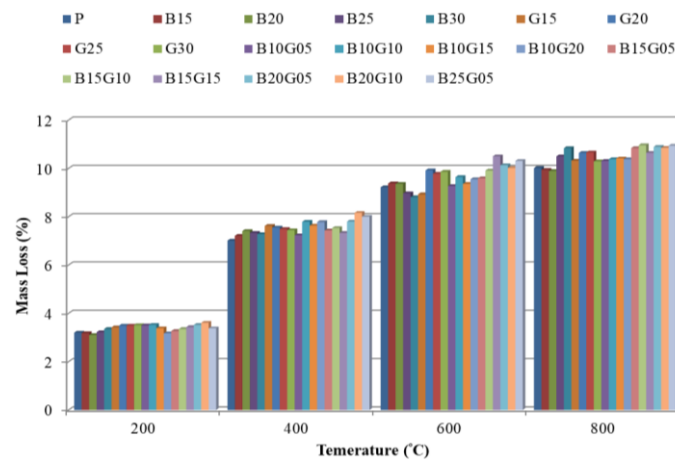


Fig. 4 Mass loss for various binary and ternary mixes of SCBA and GGBFS at elevated temperature

binary concrete containing 20% SCBA (B20 mix) at 200°C, which is 3% while the highest mass loss was observed for ternary concrete containing 15% SCBA and 10% GGBFS (B15G10) at 800°C which is 10.96%. The result shows a gradual decrease in the mass of concrete with an increase in temperature for all specimens. The initial reduction in mass may be correlated to the release of chemically bound water up to 400°C, and the final mass loss may be due to the decomposition of $\text{Ca}(\text{OH})_2$ and CSH gel (Liu *et al.* 2018).

The densities of the tested concrete are shown in Table 2. The average density of all mix proportions reduced when subjected to elevated temperature in each instance. The residual density is near to 90% of the initial density at 800°C. A decrease in density was found more for binary concrete containing SCBA than containing GGBFS. The decrement in density is due to the departure of water during heating and dehydration of hydrates (Hachemi and Ounis 2017).

3.3 UPV

The UPV measurements were performed on all 19 specimens. UPV performed on the concrete without any replacement is used as a reference to evaluate the findings gained after heating at several temperatures. The results of the UPV examination performed on 19 specimens are given in Fig. 5. The entire specimen could be categorized as a good/excellent at normal temperature and variation of 200°C for two hour heating period; their UPV was more than 3.5 km/s. At 400°C heating period for 2 h, concrete containing only 15% SCBA (B15 mix) categorized as good as its UPV greater than 3.5 km/s.

Binary concrete containing 15, 20, and 25% SCBA (B15, B20, and B25 mixes) up to 400°C shows UPV results more than 3 km/s, which are categorized as medium quality grading. All other mixes of SCBA show UPV results from less than 3 km/s, which are categorized as doubtful quality at 600°C and 800°C. Binary concrete containing 15, 20, 25, and 30% GGBFS (G15, G20, G25, and G30 mixes) at 400, 600, and 800°C shows UPV results from less than 3 km/s which are categorized as doubtful quality. Ternary concrete containing SCBA and GGBFS at 200°C shows UPV results from more than 3.5 km/s, which are categorized as good quality. Ternary concrete containing 10% SCBA & 5% GGBFS, 10% SCBA & 10% GGBFS, 10% SCBA & 15% GGBFS, 15% SCBA & 15% GGBFS and 20% SCBA & 5% GGBFS (B10G05, B10G10, B10G15, B15G15 and B20G05 mixes)

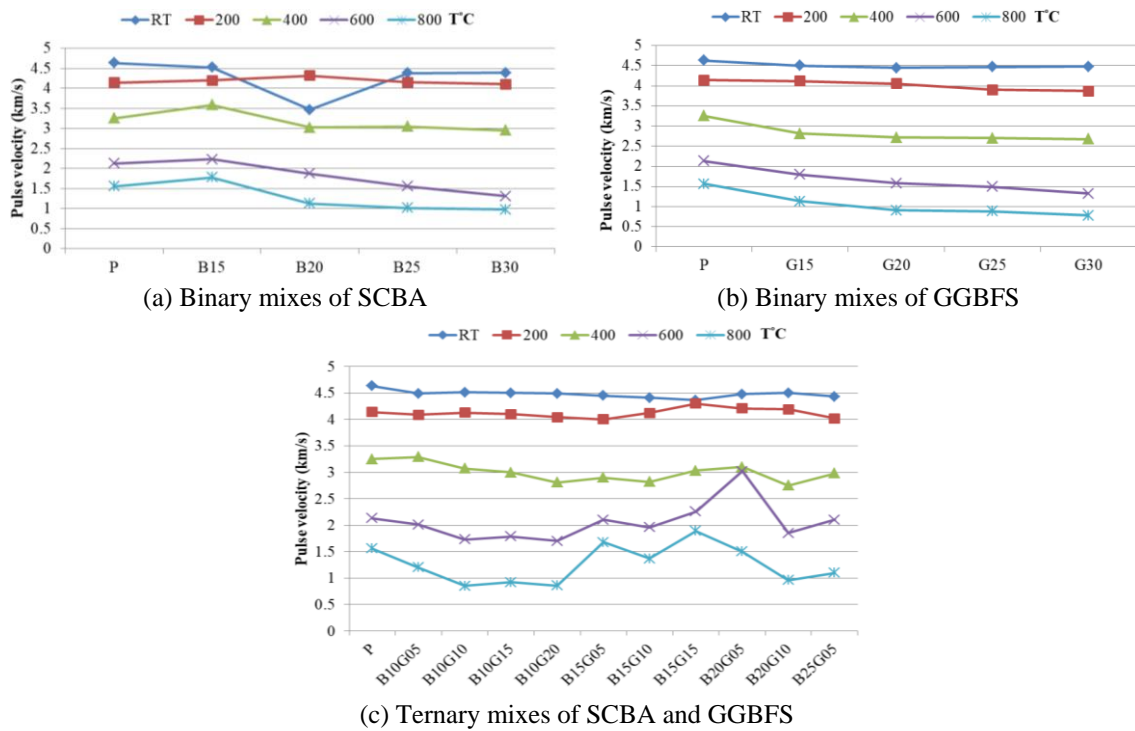


Fig. 5 Pulse velocity for various binary and ternary mixes of SCBA and GGBFS at elevated temperature

shows UPV results more than 3 km/s which are categorized as medium quality grading. At 600°C heating ternary concrete containing 20%, SCBA, and 5% GGBFS (B20G05 mix) shows UPV result of medium quality. All other ternary mixes show UPV results of doubtful quality.

UPV result of binary concrete containing 15% SCBA (B15 mix) shows improvement at water cured sample and sample at 200, 400, 600, and 800°C temperature for 2 h duration and subsequent cooling inside the furnace as compared with control concrete. The maximum standard deviation is 0.22 km/s for B15G15 mix at 600°C, for control concrete it was 0.13 km/s. After 400°C temperature, pulse velocity was found to be decreasing at a higher rate, which indicates the poor quality of material due to exposure to high temperature. Reduction in velocity from 600°C to 800°C can be attributed to the formation of cracks, which mainly increase the time required to propagate the specific distance. These outcomes can also be related to the deterioration of strength gaining components, i.e., hardened CSH gel (Sahani *et al.* 2019).

3.4 Color changes and crack appearance

After the fire hazard, the rate of deterioration of the concrete structure is examined physically without any direct test. It focuses on the visual examination of surfaces of concrete and understanding the nature of cracks developed due to high temperature. The width and depth of surface cracks give preliminary information on the severity of the deterioration due to high temperature.

The effects of increasing SCBA and GGBFS content in binary and ternary concrete on changes in cracking and color after exposure to elevated temperature are shown in Fig. 6. Visual inspection

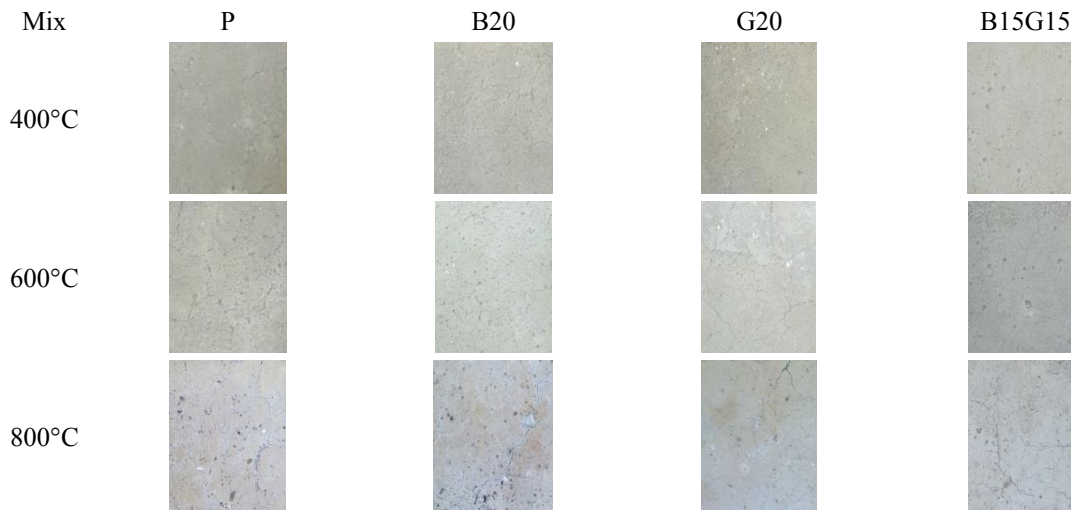


Fig. 6 Surface crack images of various binary and ternary mixes of concrete at elevated temperature

of the specimen of all concrete mixes indicated a slight change in color up to 400°C as compared to control concrete. Control concrete specimen slightly changes from its original grey color to partially reddish color at 800°C. Binary concrete containing SCBA changes its color to light brown at 800°C, whereas binary concrete containing GGBFS changes its color to white at high temperature. This color alteration is due to iron oxidation in slag particles during heating at high temperatures (Shaikh 2018).

It was difficult to identify the superimposed color resulting from grey, red, black, and white. Presence of these colors attributed to high silica content in SCBA and high lime content in GGBFS (Sahani *et al.* 2019). At 800°C, ternary mixes change to white, red, and reddish white. Hence a color change of heated concrete is primarily influenced by binding paste and mortar as it exists on the outer surface of the concrete. Overall, three types of basic changes in color changes in the specimen were observed in the concrete specimen.

It was seen that few hairline cracks are developed in control concrete at 600°C. In ternary concrete, these hairline cracks are found at 400°C, which are clearly visible at 600°C. At 800°C, hairline cracks are developed in binary concrete containing SCBA. Numbers of cracks are more in binary concrete containing GGBFS as compared with binary concrete containing SCBA. The number of cracks will go on increasing in ternary concrete at 800°C.

3.4 FESEM analysis through microstructural studies

This experiment analyses the microstructure of concrete specimens after various elevated temperatures based on the application of a scanning electron microscope (SEM). The SEM micrograph of binary and ternary concrete containing SCBA and GGBFS exposed to 400 and 800°C are shown in Fig. 7. Fig. 7(a) shows the micrographs of the reference mix and binary as well as ternary concrete at room temperature. It can be seen that at room temperature internal structure of reference concrete and concrete containing SCBA and GGBFS is dense, and the C-S-H gel exists in the form of a continuous block (Zheng *et al.* 2012). These results in higher compressive strength.

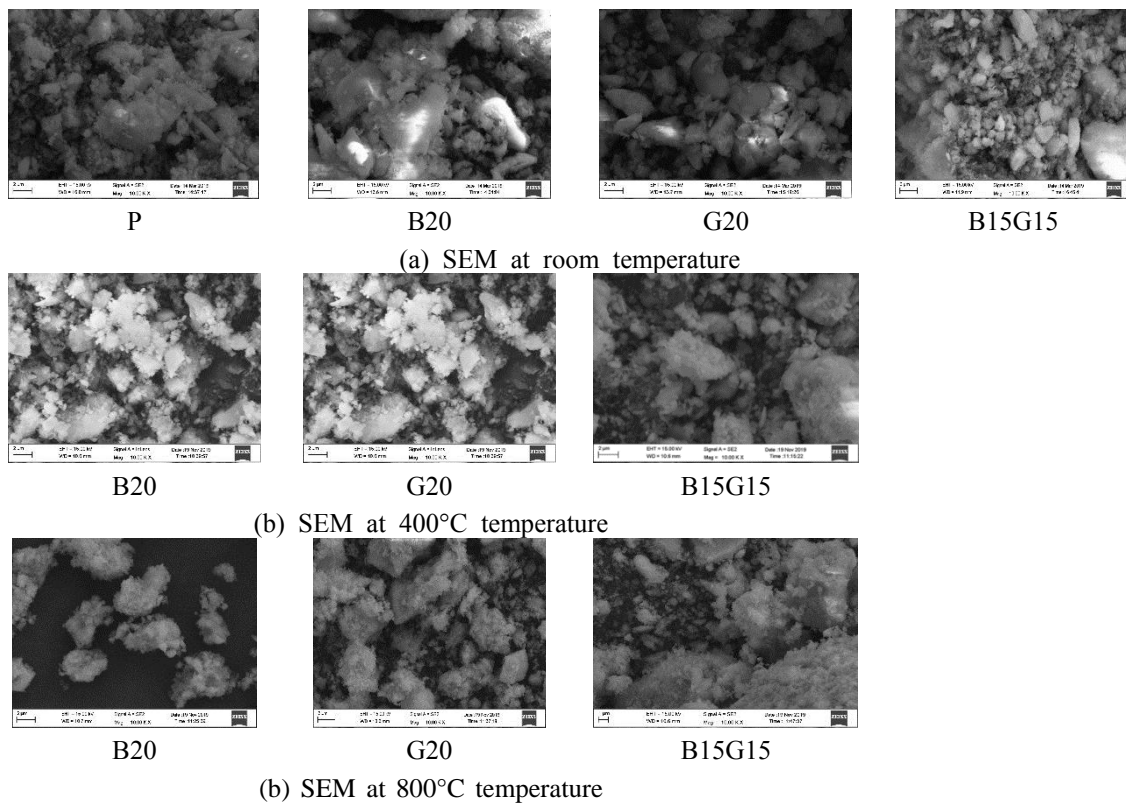


Fig. 7 SEM evaluation of the concrete specimen

When this concrete exposed to 400°C temperature, it will have the same dense internal structure, as shown in Fig. 7(b). Up to this temperature, hydration reaction accelerates and produces C-S-H gel. In case of binary concrete containing SCBA and GGBFS as shown in the figure, the C-S-H structure is perfect in which only small portion pore was observed whereas in case of binary concrete containing SCBA and GGBFS number of pores are increasing and spiked sphere appearance like coral reef was found (Tai *et al.* 2011). Up to this temperature, hydration products become cemented into continuous phase; in addition, the whole structure is more even, consequently escalating compressive strength substantially in case of binary concrete.

After exposure to 800°C, the internal structure of binary and ternary matrix present like the alveolate form (Zheng *et al.* 2012). The number of pores is going on increasing; also, the existence of complete crystal is less as compared with the 400°C temperature. At this temperature, large water vapor is generated inside the furnace due to the loss of absorbed water and pore water. At 800°C temperature, crystal water and cement hydrates initiate to dissipate. Cement hydrates usually commence to dissipate at approximately 550°C (Tai *et al.* 2011), clarifying why the concrete strength reduces enormously in this temperature span; it is mostly attributed to C-H dehydration. Fig. 7(c) shows that the microstructure loosens, a sizeable quantity of uneven rose bush like structures are seen in addition to continuous hydration product reduce in number (Tai *et al.* 2011). The influence of H on the C-H portion produced a layered plate to have several pores in addition to a rough, grainy surface.

Furthermore, several alterations were also noted in the C-S-H. A portion of it was a coral reef structure leaving behind the portion with little residual compressive strength. A portion of the coral reef structure was observed more in ternary concrete as compared with binary concrete. In binary concrete, it was noted more with concrete containing SCBA as compared with concrete containing GGBFS.

4. Conclusions

Through the experimental research on the concrete modified with SCBA and GGBFS after heating for temperature up to 800°C, the following conclusions are drawn:

- Compressive strength enhanced in binary concrete containing SCBA (SiO₂ content was 82.53%) for B15 mix and in concrete containing GGBFS (CaO content was 35.46%) for G15 and G20 mix. Microstructural studies indicate that extra C-S-H gel was found in concrete containing GGBFS. For all combinations, compressive strength rises till 400°C but starts to fall as temperature increases continuously. SEM image shows dense structure up to 400°C, which improves compressive strength; beyond these temperatures, coral leaf structure was observed where strength decreases. B15 mix has higher compressive strength among all combinations at all temperatures.
- Higher heating temperature led to higher mass loss, and this effect is higher up to 400°C temperature and becomes irrelevant subsequently. Mass loss was more for GGBFS as compare with SCBA; this may be due to the decomposition of Ca(OH)₂ and C-S-H gel.
- The UPV of concrete declines with the rise in temperature, and the rate of decline accelerates from 400°C onwards. Concrete containing GGBFS presents lower values when compared with concrete containing SCBA.
- After exposure to elevated temperature binary and ternary concrete loses its density, color changes and development of cracks were observed. Cracks are more in concrete containing GGBFS as compared with SCBA.
- SCBA is better for concrete subjected to elevated temperature as compared with GGBFS as SCBA based concrete shows better performance in terms of compressive strength, mass loss, density, and UPV. However, ternary concrete incorporating SCBA and GGBFS (B10G05 & B10G10 mix) also shows better performance at elevated temperatures.

References

- Arioz, O. (2007), "Effects of elevated temperatures on properties of concrete", *Fire Safety J.*, **42**(8), 516-522.
<https://doi.org/10.1016/j.firesaf.2007.01.003>
- Ashteyat, A.M., Haddad, R.H. and Ismeik, M. (2014), "Prediction of mechanical properties of post-heated self-compacting concrete using non-destructive tests", *Eur. J. Environ. Civil Eng.*, **18**(1), 1-10.
<https://doi.org/10.1080/19648189.2013.841593>
- Belouadah, M., Rahmouni, Z.E.A. and Tebbal, N. (2018), "Effects of glass powder on the characteristics of concrete subjected to high temperatures", *Adv. Concrete Constr., Int. J.*, **6**(3), 311-322.
<https://doi.org/10.12989/acc.2018.6.3.311>
- Chan, Y.N., Luo, X. and Sun, W. (2000), "Compressive strength and pore structure of high-performance concrete after exposure to high temperature up to 800°C", *Cement Concrete Res.*, **30**(2), 247-251.

- [https://doi.org/10.1016/S0008-8846\(99\)00240-9](https://doi.org/10.1016/S0008-8846(99)00240-9)
- Chen, Z., Chen, J., Ning, F. and Li, Y. (2019), "Residual properties of recycled concrete after exposure to high temperatures", *Magazine Concrete Res.*, **71**(15), 781-793. <https://doi.org/10.1680/jmacr.17.00503>
- Deshpande, A.A., Kumar, D. and Ranade, R. (2019), "Influence of high temperatures on the residual mechanical properties of a hybrid fiber-reinforced strain-hardening cementitious composite", *Constr. Build. Mater.*, **208**, 283-295. <https://doi.org/10.1016/j.conbuildmat.2019.02.129>
- Dong, X., Ding, Y. and Wang, T. (2008), "Spalling and mechanical properties of fiber reinforced high-performance concrete subjected to fire", *J. Wuhan Univ. Technol., Materials Science Edition*, **23**(5), 743-749. <https://doi.org/10.1007/s11595-007-5743-5>
- Drzymala, T., Jackiewicz-Rek, W., Tomaszewski, M., Kus, A., Galaj, J. and Sukys, R. (2017), "Effects of High Temperature on the Properties of High Performance Concrete (HPC)", *Procedia Eng.*, **172**, 256-263. <https://doi.org/10.1016/j.proeng.2017.02.108>
- Drzymala, T., Jackiewicz-Rek, W., Galaj, J. and Sukys, R. (2018), "Assessment of mechanical properties of high strength concrete (HSC) after exposure to high temperature", *J. Civil Eng. Manage.*, **24**(2), 138-144. <https://doi.org/10.3846/jcem.2018.457>
- Gencil, O., Brostow, W., Del Coz Diaz, J.J., Martínez-Barrera, G. and Beycioglu, A. (2013), "Effects of elevated temperatures on mechanical properties of concrete containing haematite evaluated using fuzzy logic model", *Mater. Res. Innov.*, **17**(6), 382-391. <https://doi.org/10.1179/1433075X12Y.0000000070>
- Hachemi, S. and Ounis, A. (2017), "The influence of sand nature on the residual physical and mechanical properties of concrete after exposure to elevated temperature", *Eur. J. Environ. Civil Eng.*, **8189**(May), 1-16. <https://doi.org/10.1080/19648189.2017.1327893>
- Hewlett, P.C. (2004), *Lea's Chemistry of Cement and Concrete*, Elsevier Butterworth Heinemann Publication, Oxford, UK.
- IS 10262 (2009), Recommended guidelines for concrete mix design, Bureau of Indian Standards, New Delhi, India.
- IS 12269 (1987), Specification for ordinary Portland cement, Bureau of Indian Standards, New Delhi, India.
- IS 13311(Part I) (1992), Non-destructive testing of concrete-Methods of test for Ultrasonic pulse velocity, Bureau of Indian Standards, New Delhi, India.
- IS 383 (1970), Specification for coarse and fine aggregates from natural sources for concrete, Bureau of Indian Standards, New Delhi, India.
- IS 4031(Part 5) (1988), Methods of physical tests for hydraulic cement: Determination of initial and final setting times, Bureau of Indian Standards, New Delhi, India.
- IS 456 (2000), Code of practice for plain and reinforced concrete, Bureau of Indian Standards, New Delhi, India.
- IS 516 (1959), Method of tests for strength of concrete, Bureau of Indian Standards, New Delhi, India.
- ISO/TR 15655 (2003), Fire resistance-test for thermo-physical and mechanical properties of structural materials at elevated temperatures for fire engineering design, Technical report; Geneva, Switzerland.
- Khan, M.S. and Abbas, H. (2016), "Performance of concrete subjected to elevated temperature", *Eur. J. Environ. Civil Eng.*, **20**(5), 532-543. <https://doi.org/10.1080/19648189.2015.1053152>
- Ko, J., Ryu, D. and Noguchi, T. (2011), "The spalling mechanism of high-strength concrete under fire", *Magaz. Concrete Res.*, **63**(5), 357-370. <https://doi.org/10.1680/mac.10.00002>
- Le, Q.X., Dao, V.T.N., Torero, J.L., Maluk, C. and Bisby, L. (2018), "Effects of temperature and temperature gradient on concrete performance at elevated temperatures", *Adv. Struct. Eng.*, **21**(8), 1223-1233. <https://doi.org/10.1177/1369433217746347>
- Liu, Y., Jin, B., Huo, J. and Li, Z. (2018), "Effect of microstructure evolution on mechanical behaviour of concrete after high temperatures", *Magaz. Concrete Res.*, **70**(15), 770-784. <https://doi.org/10.1680/jmacr.17.00197>
- Ma, Q., Guo, R., Sun, Y., He, K., Du, H., Yan, F., Lin, Z. and Zhao, Z. (2018), "Behaviour of modified lightweight aggregate concrete after exposure to elevated temperatures", *Magaz. Concrete Res.*, **70**(5), 217-230. <https://doi.org/10.1680/jmacr.17.00136>
- Ozawa, M. and Morimoto, H. (2014), "Effects of various fibres on high-temperature spalling in high-

- performance concrete”, *Constr. Build. Mater.*, **71**, 83-92.
<https://doi.org/10.1016/j.conbuildmat.2014.07.068>
- Poon, C.S., Shui, Z.H. and Lam, L. (2004), “Compressive behavior of fiber reinforced high-performance concrete subjected to elevated temperatures”, *Cement Concrete Res.*, **34**(12), 2215-2222.
<https://doi.org/10.1016/j.cemconres.2004.02.011>
- Sahani, A.K., Samantaa, A.K. and Roy, D.K.S. (2019), “Influence of mineral by-products on compressive strength and microstructure of concrete at high temperature”, *Adv. Concrete Constr., Int. J.*, **7**(4), 263-275.
<https://doi.org/10.12989/acc.2019.7.4.263>
- Salau, M.A., Oseafiana, O.J. and Oyegoke, T.O. (2015), “Effects of elevated temperature on concrete with Recycled Coarse Aggregates”, *Proceedings of IOP Conference Series: Materials Science and Engineering*, **96**(1). <https://doi.org/10.1088/1757-899X/96/1/012078>
- Shaikh, F.U.A. (2018), “Effects of slag content on the residual mechanical properties of ambient air-cured geopolymers exposed to elevated temperatures”, *J. Asian Ceramic Societies*, **6**(4), 342-358.
<https://doi.org/10.1080/21870764.2018.1529013>
- Siddique, R. and Kaur, D. (2012), “Properties of concrete containing ground granulated blast furnace slag (GGBFS) at elevated temperatures”, *J. Adv. Res.*, **3**(1), 45-51. <https://doi.org/10.1016/j.jare.2011.03.004>
- Sideris, K.K., Manita, P. and Chaniotakis, E. (2009), “Performance of thermally damaged fibre reinforced concretes”, *Constr. Build. Mater.*, **23**(3), 1232-1239. <https://doi.org/10.1016/j.conbuildmat.2008.08.009>
- Tai, Y.S., Pan, H.H. and Kung, Y.N. (2011), “Mechanical properties of steel fiber reinforced reactive powder concrete following exposure to high temperature reaching 800°C”, *Nuclear Eng. Des.*, **241**(7), 2416-2424.
<https://doi.org/10.1016/j.nucengdes.2011.04.008>
- Wu, Z., Lo, S.H., Kang, H.T. and Su, K.L. (2019), “High Strength Concrete Tests under Elevated Temperature”, *Athens J. Technol. Eng.*, **6**(3), 141-162. <https://doi.org/10.30958/ajte.6-3-1>
- Yadollahi, M.M., Benli, A. and Demirboğa, R. (2015), “Effects of elevated temperature on pumice based geopolymer composites”, *Plast. Rubber Compos.*, **44**(6), 226-237.
<https://doi.org/10.1179/1743289815Y.0000000020>
- Zhao, H., Wang, Y. and Liu, F. (2017), “Stress-strain relationship of coarse RCA concrete exposed to elevated temperatures”, *Magaz. Concrete Res.*, **69**(13), 649-664. <https://doi.org/10.1680/jmacr.16.00333>
- Zheng, W., Li, H. and Wang, Y. (2012), “Compressive behaviour of hybrid fiber-reinforced reactive powder concrete after high temperature”, *Mater. Des.*, **41**, 403-409. <https://doi.org/10.1016/j.matdes.2012.05.026>